PROCEEDINGS OF SCIENCE

Low-Power Radiofrequency Systems for the RNO-G Project

E. Oberla[a,*] **for the RNO-G Collaboration**
(a complete list of authors can be found at the end of the proceedings)

[a] *University of Chicago,*
5640 S. Ellis Ave, Chicago, USA
E-mail: ejo@uchicago.edu

The Radio Neutrino Observatory in Greenland (RNO-G) seeks to detect the Askaryan radio emission from energetic neutrinos (> 10 PeV) interacting in the Greenland ice sheet. The RNO-G detector comprises an array of independent and autonomous radio-detector stations, each with a hybrid design composed of deep borehole (~100m) and surface antennas, which require low-power, robust, and scalable low-noise radiofrequency (RF) amplifier and signal-transport systems over a ~80-650MHz bandwidth. In this contribution, we will present the design and performance of the custom RNO-G RF signal chains, including a field-proven and low-cost RF-over-fiber (RFoF) unit.

The 38th International Cosmic Ray Conference (ICRC2023)
26 July – 3 August, 2023
Nagoya, Japan

*Speaker

PoS(ICRC2023)1171

1. Introduction

The Radio Neutrino Observatory in Greenland (RNO-G) is a distributed-station array targeting the detection of ultra-high energy neutrinos, searching for the ensuant broadband radio (Askaryan) emission from the interactions of these cosmic neutrinos in glacial ice. RNO-G, currently under construction near Summit Station, Greenland, comprises both deep in-borehole (~100 m) and near-surface antennas with a receiving bandwidth of ~80-650 MHz, and 24 such antenna-receiver channels per station [1]. The RNO-G detector systems are designed with the ability to scale, to be robust for long-term operation in harsh conditions, and to meet the project science goals at the lowest possible power in order to operate autonomously using renewable-energy power sources.

The active radiofrequency (RF) signal chains are one of these RNO-G detector systems, and their design and performance are the subject of these Proceedings. For maximum sensitivity, the RF system is required to be 'ice-noise' dominated in the deep receivers; this noise is black-body (thermal) radiation from the ~240 K ice that fills the beam of the borehole antennas. Over the RNO-G bandwidth, this amounts to a noise power of ~2 pW and is the irreducible single-antenna noise background near which the RNO-G detector is searching for the broadband (few ~ns time-domain duration) Askaryan signals.

The custom RF signal chains are responsible for bringing these diminutive signals to a measurable level for conventional digitizers, while adding minimal electronics noise or distortion. With the instrumental challanges and constraints, the signal chains are fully custom as commercially available options did not work within the specifications. The deep borehole antennas are equipped with a custom RF-over-fiber (RFoF) implementation for long-distance signal transport and the near-surface receivers use a custom highly-integrated circuit board. The RNO-G detector also incorporates several RF calibration transmitters that will be described, along with the RF receiving systems, in the following Sections.

2. Design

2.1 Deep Receivers: IGLU & DRAB

The RF signal-chain for the RNO-G in-ice receivers is composed of two units: the In-ice Gain with Low-noise Unit (IGLU), which installs directly above its counterpart borehole antenna, and the Downhole Receiver and Amplifier Board (DRAB), which is a quad-channel board that sits in the main instrument enclosure installed at the surface. The IGLU and DRAB boards, pictured in Fig 1, include a custom low-power RFoF design to transport the deep-antenna signals ~100 m to the surface instrument box. The use of bulky coaxial cables for signal transport was not feasible, both for deployment practicalities and for the induced noise and spectral features over such cable lengths.

A block diagram of the in-ice RF chain is shown in Fig 2. The LNA used is the Infineon BGB741L7ESD, which is biased at 10 mA, and is matched at the input and output to a 50Ω characteristic impedance. The system bandpass is defined with filters in two locations, both on the IGLU and DRAB. A high-isolation RF amplifier is used following the IGLU bandpass filter to aid in the impedance matching to the laser diode. This amplifier has high in-band 'active directivity' (|S12(dB)| - S21(dB) > 10dB).

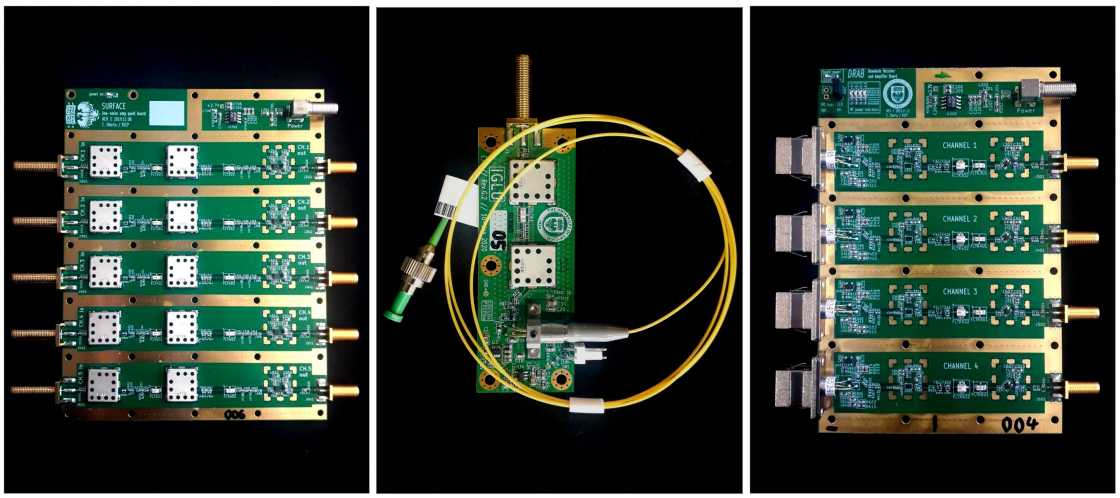

Figure 1: RF signal-chain boards for the RNO-G receivers. Left: Fully integrated five-channel Surface receiver board for the near-surface antenna signals via coaxial cable. Middle: an IGLU board, with a first-stage LNA and a second-stage circuit to convert the electrical signal to optical for transport over fiber. Right: The DRAB quad-channel unit to receive the optical signal from the IGLUs and convert back to an electrical signal, with additional RF conditioning. The boards are all shown without their plated-aluminum RF enclosures.

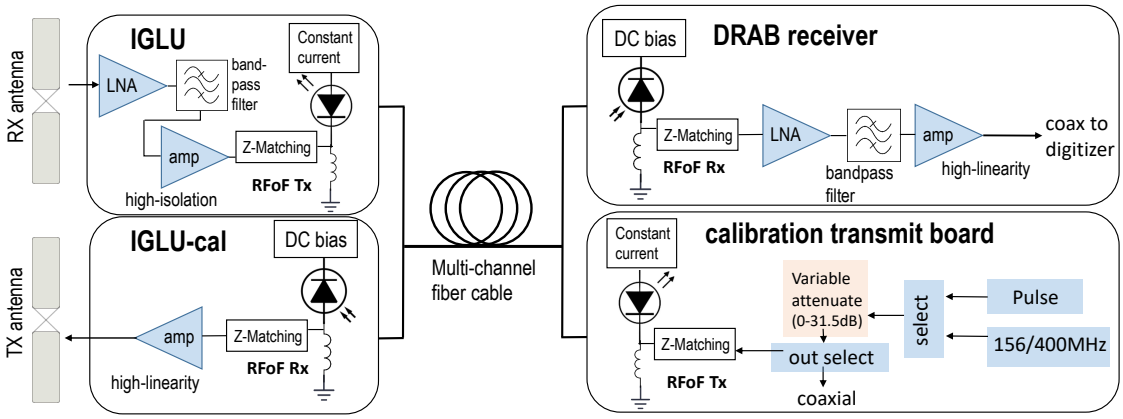

Figure 2: Block diagram of the downhole receiver and calibration-transmit systems. On the left are the in-ice IGLU and IGLU-cal units, which interface to the DRAB receivers and Calibration Transmitter board in the surface instrument box over 4- or 6-channel fiber cables.

The RFoF transmitter is designed as a directly-modulated laser diode, in which the RF signal modulates the laser optical intensity. This is a simple and robust electrical-to-optical conversion that works well at low RF signal powers, partially inspired by the custom links developed by CHIME and other radioastronomy observatories [2, 3]. An economical Fabry-Perot laser diode (FPMR3 AGx Technologies) at 1310 nm is used and has now been well qualified in operation down to -50C in the boreholes, and is viable laser for optical signal transport less than a few hundred meters [4]. Laser diodes are more efficient at cold temperatures, so the IGLU laser can be driven at a relatively low bias current of 16mA that still holds the device sufficiently above the lasing threshold at the cold, but stable, borehole temperatures.

The IGLU enclosure has a FC/APC simplex fiber adapter, that is connected in the field to the long fiber runs to the surface during deployment. Military-rated single mode fiber is used for both the short staggered simplex fiber lengths connected to each IGLU, and the bulk multi-channel fiber cable used over the full vertical extent of the borehole to the surface instrument box. These fibers are rated for installation down to -55C and have robust impact-resistance and bend-radius ratings.

At the surface, the fiber bundle connects to the main instrument that feeds the signal to the DRAB receivers. These boards use optically broadband reversed-biased photodiodes, which are integrated into either an FC/APC or SC/APC connector (SC/APC shown in Fig. 1). The electrical output is passed through two further amplifiers, intermediated with a last bandpass-defining stage, to drive a 50Ω short coaxial cable to the RNO-G digitization and triggering systems.

2.2 Surface Receivers

The 5-channel Surface receiver board, pictured in Fig 1, is a fully electrical RF signal-chain that uses many similar components as the IGLU-DRAB deep receiver. The Surface signal chain employs the same LNA->filter->amp->filter->amp design that is used on the input-side of the IGLU and the output side of the DRAB. The RNO-G near-surface antennas are routed to the instrument box using 11m LMR400 coaxial cables, which connect directly to the pair of Surface RF boards. As the near-surface antennas are more subjected to RFI (land-mobile radios, etc), the Surface receivers have a power-limiter installed on the input to reflect large RF signals (>0dBm) at the input, in order to protect the signal chain.

The Surface receiver board is a highly-compact RF unit with >60dB of gain per channel with closely-packed channels. To maximize performance, the board is housed in a machined shield, with milled 'pockets' isolating each channel. Adhesive RF-absorber is placed in each pocket to dampen potential cavity resonances. The nearest-neighbor crosstalk rejection is measured at better than 85dB across the band with this shielding configuration.

2.3 Calibration Transmitters

The RNO-G station design includes two deep calibration transmitter antennas, which provide various controlled signal outputs to interrogate the receiving array. These transmitters are designed as the RFoF reverse path to the IGLU-DRAB, as shown in Fig. 2, in which the Calibration Transmit Board houses the RFoF laser diode and the in-ice IGLU-cal receives the optical signal and converts to an electrical-RF impulse presented to the transmit antenna. The Calibration Transmit laser diodes are biased at much higher current, 50-60mA, to ensure good operation of the laser and to accommodate larger signal-modulation amplitudes. The receive and transmit optical signals are combined on the same multi-channel fiber cable used for each borehole to simplify antenna-string deployment.

The Calibration Transmit board includes a fast-impulse, which stimulates a neutrino-like radio transient in the receivers, and two continuous-wave sinuous signals at 156.25 and 400MHz. In future iterations, a calibrated noise-diode will be included to aid in absolute amplitude calibrations at the receivers. The waveform can be variably attenuated over a wide 30dB range, which allows the *in situ* trigger efficiency to be measured near the ~2 pW thermal-noise threshold, for example. Four output paths are selectable: the two downhole RFoF paths, or two coaxial paths used for a near-surface

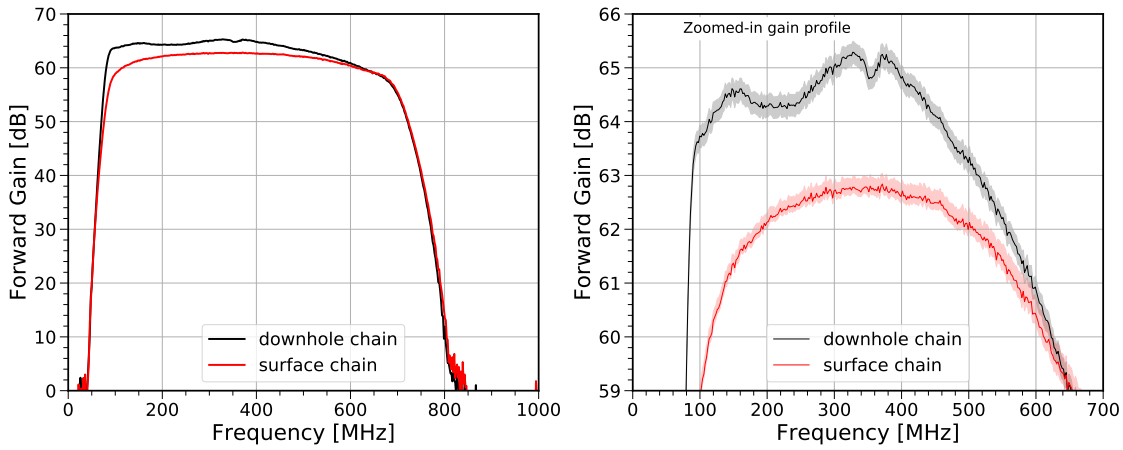

Figure 3: Forward gain of the RNO-G RF receiving chains. The left figure shows the full gain profile for the two chains. On the right, the vertical axis is zoomed-in to the primary in-band gain, with shaded region outlining the temperature dependence described in the text.

transmitter or a reference RF signal within the instrument box. The waveform source, attenuation, and output-path selection are controlled over a serial I2C interface to the main instrument-controller board, and the fast impulse can be synchronized to the GPS pulse-per-second.

2.4 Power Consumption

The main RNO-G instrument provides a 3.3V rail from a dedicated high-efficient and highly-filtered DC-DC switching regulator for the RF subsystems. The local operating voltage at each RF board is either 2.5 or 2.7 V, supplied by an on-board linear regulator that down-converts the 3.3V input rail (point-of-load regulation). Each borehole string and each DRAB, Surface, and Calibration Transmit board has an independent power switch within the instrument box for discrete enable/disable and current monitoring. Referenced to the primary 3.3V voltage rail, the power draws of the boards are the following: IGLU (150mW, single-channel), IGLU-cal (90mW, single-channel), DRAB (450mW, quad-channel), and Surface (710mW, five-channels). The Calibration Transmitter board can draw up to 800mW when enabled, but is only powered when a calibration cycle is active. The total 24-channel RF system power draw, including an additional unused SURFACE and DRAB channel each, is about 5.6 W.

3. Performance

3.1 Gain

The forward gain of the two receiving signal chains is shown in Fig. 3. An in-band gain of greater than 60dB is required to bring the thermal-noise floor to a level that can be readily digitized with a resolution of a few bits, which is 5-10 mVrms. The RNO-G stations communicate wirelessly over LTE and LoRaWAN networks, at 850-950MHz, so good RF rejection is also required and demonstrated (>70dB) at these frequencies. The -3dB bandwidth is 85-570MHz and 105-605MHz

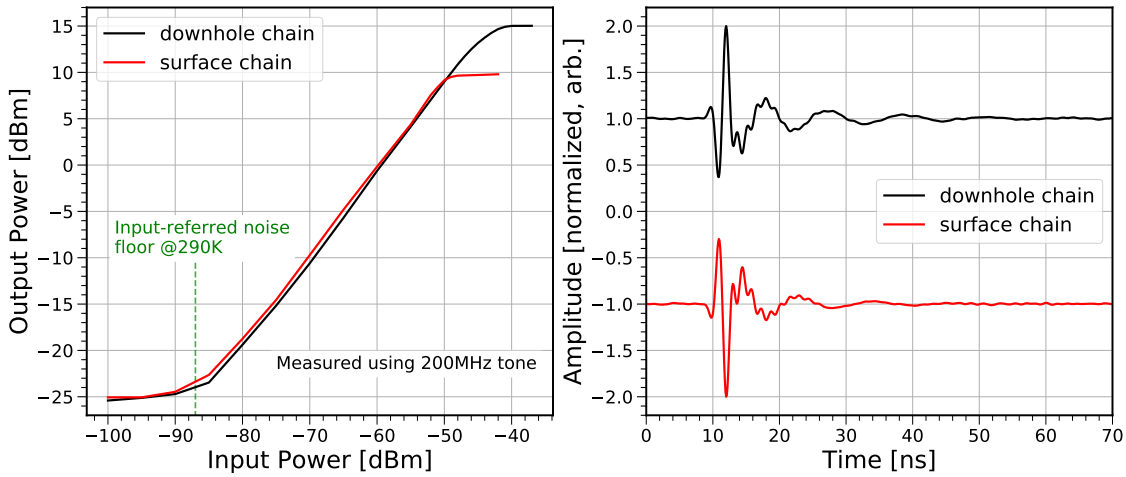

Figure 4: Dynamic range performance, left, and signal-chain impulse response, right.

for the downhole and surface RF chains, respectively. Both chains have a ~80-650MHz range if using a -6dB bandwidth definition. The antenna response is not included here.

The stability of the gain profile over temperature is shown on the right in Fig. 3. For the downhole gain-profile measurement, the IGLU is kept at a constant -40C and the DRAB is varied between -20C and 20C. The surface chain is similarly varied between -20C and 20C, which is the typical extents of the amplifiers in the surface instrument box when in operation. In both cases, the gain profile is stable to better than 0.5dB.

3.2 Dynamic Range and Impulse Response

A wide dynamic range is important for the RF signal chains, as signals-of-interest may have incident powers much greater than the thermal-noise level. The measured dynamic range, using a 200MHz tone generated by a HP8648B signal generator, is shown on the left in Fig 4, with a room temperature noise floor of ~-87dBm (this will be closer to -88dBm in-ice). The input-referred 1dB compression point is measured to be -46dBm and -53dBm for the downhole and surface chains, respectively. Thus, the dynamic range for the two chains, referenced to the noise floor, is 41dB and 34dB, respectively. The downhole chain is well-matched to the digitizer range, and, while the surface chain slightly under-performs, it is sufficient. A prior version of the surface chain matched the downhole chain in range, but was swapped for a chain with slightly higher gain, sacrificing somewhat in this metric.

The time-domain impulse response for the two RF signal chains is shown on the right in Fig. 4. This measurement was performed using a 140ps FWHM impulse, which has a flat gain profile out to 3GHz. No deconvolution was therefore required or performed on these data. Both signal chains show a snappy impulse with minimal obvious reflections, which is a confirmation on the good impedance match to a 50Ω input and output. Most of the signal power is contained in the first ~8ns in both chains.

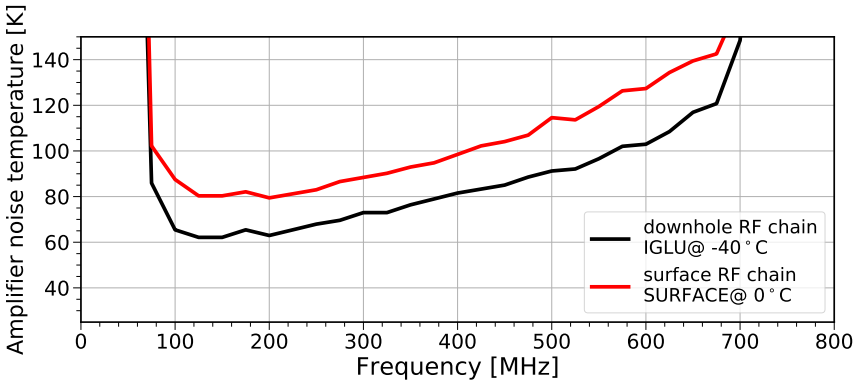

Figure 5: Noise temperature of the two signal chains.

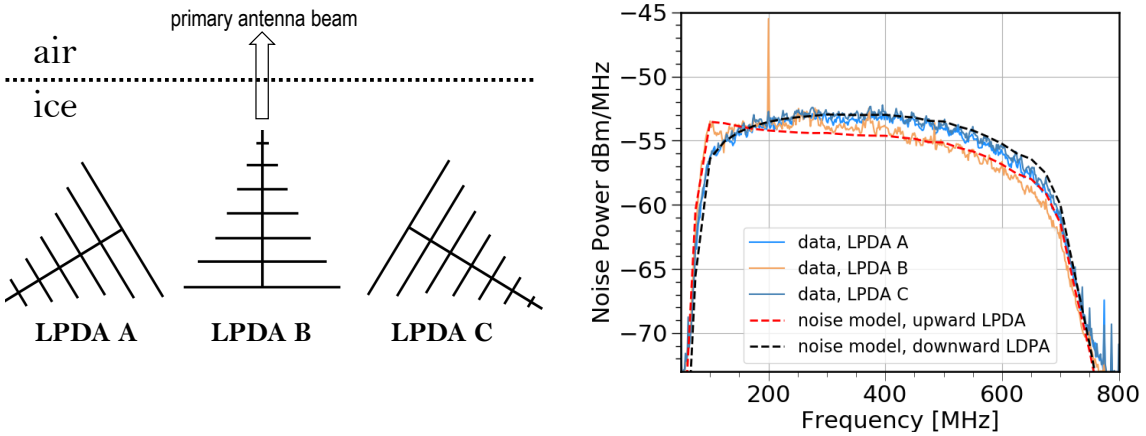

Figure 6: The surface LPDA installation, left, and the noise power spectral density, right, both measured and modeled for the different LPDA orientations.

3.3 Noise

A primary requirement of the RF systems is to be a sub-dominant noise source in comparison to the ~240K ice that is viewed by the deep in-ice antennas. The noise temperature of the two chains, measured using an HP8970B noise-figure meter equipped with a 346A 5dB-ENR calibrated noise-source, is shown in Fig. 5. For this measurement, the IGLU was held at -40C and the Surface board at 0C. Both chains have noise temperatures significantly less than the thermal-noise temperature of the ice across the band. In particular, the downhole chain has an average noise contribution of only 70K in the 80-250MHz trigger-band used for RNO-G.

The noise performance can also be validated using the RNO-G near-surface log-periodic dipole antennas (LPDAs), installed in a ternary orientation as shown in Fig. 6. These are directional antennas, such that the (frequency-dependent) beam points along the indicated axis. With a simplified model, we assume that the downward LPDAs view only the thermal noise from the ice, while the upward LPDA will see some combination of the ice and sky temperatures, taken to be 50% of each, with the sky noise dominated by the galactic radio emission at these frequencies and characterized by the functional form in [5]. The Surface amplifier noise temperature, as measured above, is included in both and then the models are convolved with the forward-gain curve shown in

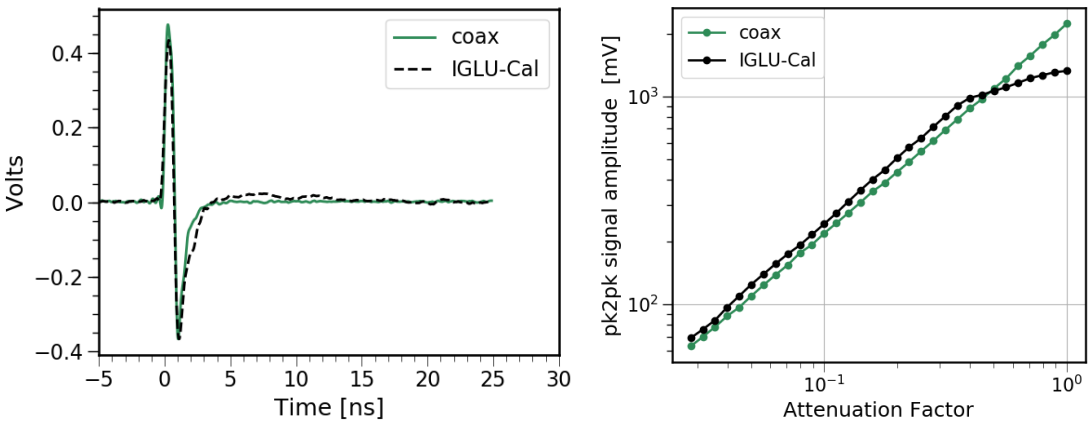

Figure 7: The impulse output waveforms, on both the RFoF and coaxial paths, and the dynamic range of the calibration RF system.

Fig. 3. The measured spectra, taken from unbiased-triggered events in a typical 2-hr RNO-G data acquisition run, are distinct between the upward- and downward-pointing LPDAs, and the simple models for each LPDA direction matches the observations well.

3.4 Calibration Transmitter

The generated fast-impulse waveforms for both the deep RFoF and the coaxial-output calibration transmitters are shown in Fig 7. The impulse, as presented to an antenna, is generated by differentiating a sub-ns generated unipolar pulse and matches the bandwidth of the receiving antenna system well.

The transmitter output amplitude is controlled with a digitally-controlled step-attenuator on the Calibration Transmit board. The downhole RFoF transmitter starts to compress around 1 Vpp (13dBm) signals into the borehole transmit antenna, limited in combination by the laser diode modulation and the final-stage restoration amplifier on the IGLU-cal. The coaxial output path, which has neither of these components, is linear across the full dynamic range.

4. Conclusion

The custom RF system design and performance for the RNO-G project are described. This highly-integrated and low-power system is field-proven, providing robust and high-fidelity RF signal conditioning, and the design principles are applicable to other fielded RF systems.

References

[1] **RNO-G** Collaboration, J. A. Aguilar *et al.* *JINST* **16** no. 03, (2021) P03025. [Erratum: JINST 18, E03001 (2023)].

[2] J. Mena *et al.* *JINST* **8** (2013) .

[3] J. Welch *et al.* *Proceedings of the IEEE* **97** no. 8, (2009) .

[4] J. Capmany *et al.* *Journal of the Optical Society of America B* **22** no. 10, (2005) .

[5] S. Ellingson *IEEE Transactions on Antennas and Propagation* **53** no. 8, (2005) .

Full Author List: RNO-G Collaboration

J. A. Aguilar[1], P. Allison[2], D. Besson[3], A. Bishop[10], O. Botner[4], S. Bouma[5], S. Buitink[6], W. Castiglioni[8], M. Cataldo[5], B. A. Clark[7], A. Coleman[4], K. Couberly[3], P. Dasgupta[1], S. de Kockere[9], K. D. de Vries[9], C. Deaconu[8], M. A. DuVernois[10], A. Eimer[5], C. Glaser[4], T. Glüsenkamp[4], A. Hallgren[4], S. Hallmann[11], J. C. Hanson[12], B. Hendricks[14], J. Henrichs[11,5], N. Heyer[4], C. Hornhuber[3], K. Hughes[8], T. Karg[11], A. Karle[10], J. L. Kelley[10], M. Korntheuer[1], M. Kowalski[11,15], I. Kravchenko[16], R. Krebs[14], R. Lahmann[5], P. Lehmann[5], U. Latif[9], P. Laub[5], C.-H. Liu[16], J. Mammo[16], M. J. Marsee[17], Z. S. Meyers[11,5], M. Mikhailova[3], K. Michaels[8], K. Mulrey[13], M. Muzio[14], A. Nelles[11,5], A. Novikov[19], A. Nozdrina[3], E. Oberla[8], B. Oeyen[18], I. Plaisier[5,11], N. Punsuebsay[19], L. Pyras[11,5], D. Ryckbosch[18], F. Schlüter[1], O. Scholten[9,20], D. Seckel[19], M. F. H. Seikh[3], D. Smith[8], J. Stoffels[9], D. Southall[8], K. Terveer[5], S. Toscano[1], D. Tosi[10], D. J. Van Den Broeck[9,6], N. van Eijndhoven[9], A. G. Vieregg[8], J. Z. Vischer[5], C. Welling[8], D. R. Williams[17], S. Wissel[14], R. Young[3], A. Zink[5]

[1] Université Libre de Bruxelles, Science Faculty CP230, B-1050 Brussels, Belgium
[2] Dept. of Physics, Center for Cosmology and AstroParticle Physics, Ohio State University, Columbus, OH 43210, USA
[3] University of Kansas, Dept. of Physics and Astronomy, Lawrence, KS 66045, USA
[4] Uppsala University, Dept. of Physics and Astronomy, Uppsala, SE-752 37, Sweden
[5] Erlangen Center for Astroparticle Physics (ECAP), Friedrich-Alexander-Universität Erlangen-Nürnberg, 91058 Erlangen, Germany
[6] Vrije Universiteit Brussel, Astrophysical Institute, Pleinlaan 2, 1050 Brussels, Belgium
[7] Department of Physics, University of Maryland, College Park, MD 20742, USA
[8] Dept. of Physics, Enrico Fermi Inst., Kavli Inst. for Cosmological Physics, University of Chicago, Chicago, IL 60637, USA
[9] Vrije Universiteit Brussel, Dienst ELEM, B-1050 Brussels, Belgium
[10] Wisconsin IceCube Particle Astrophysics Center (WIPAC) and Dept. of Physics, University of Wisconsin-Madison, Madison, WI 53703, USA
[11] Deutsches Elektronen-Synchrotron DESY, Platanenallee 6, 15738 Zeuthen, Germany
[12] Whittier College, Whittier, CA 90602, USA
[13] Dept. of Astrophysics/IMAPP, Radboud University, PO Box 9010, 6500 GL, The Netherlands
[14] Dept. of Physics, Dept. of Astronomy & Astrophysics, Penn State University, University Park, PA 16801, USA
[15] Institut für Physik, Humboldt-Universität zu Berlin, 12489 Berlin, Germany
[16] Dept. of Physics and Astronomy, Univ. of Nebraska-Lincoln, NE, 68588, USA
[17] Dept. of Physics and Astronomy, University of Alabama, Tuscaloosa, AL 35487, USA
[18] Ghent University, Dept. of Physics and Astronomy, B-9000 Gent, Belgium
[19] Dept. of Physics and Astronomy, University of Delaware, Newark, DE 19716, USA
[20] Kapteyn Institute, University of Groningen, Groningen, The Netherlands

Acknowledgments

We are thankful to the staff at Summit Station for supporting our deployment work in every way possible. We also acknowledge our colleagues from the British Antarctic Survey for embarking on the journey of building and operating the BigRAID drill for our project. We would like to acknowledge our home institutions and funding agencies for supporting the RNO-G work; in particular the Belgian Funds for Scientific Research (FRS-FNRS and FWO) and the FWO programme for International Research Infrastructure (IRI), the National Science Foundation (NSF Award IDs 2118315, 2112352, 211232, 2111410) and the IceCube EPSCoR Initiative (Award ID 2019597), the German research foundation (DFG, Grant NE 2031/2-1), the Helmholtz Association (Initiative and Networking Fund, W2/W3 Program), the University of Chicago Research Computing Center, and the European Research Council under the European Unions Horizon 2020 research and innovation programme (grant agreement No 805486).